Supporting Information

A gel-free $Ti_3C_2T_x$-based electrode array for high-density, high-resolution surface electromyography

*Brendan B. Murphy, Patrick J. Mulcahey, Nicolette Driscoll, Gregory T. Robbins, Andrew G. Richardson, Nicholas V. Apollo, Kathleen Maleski, Timothy H. Lucas, Yury Gogotsi, Timothy Dillingham, & Flavia Vitale**

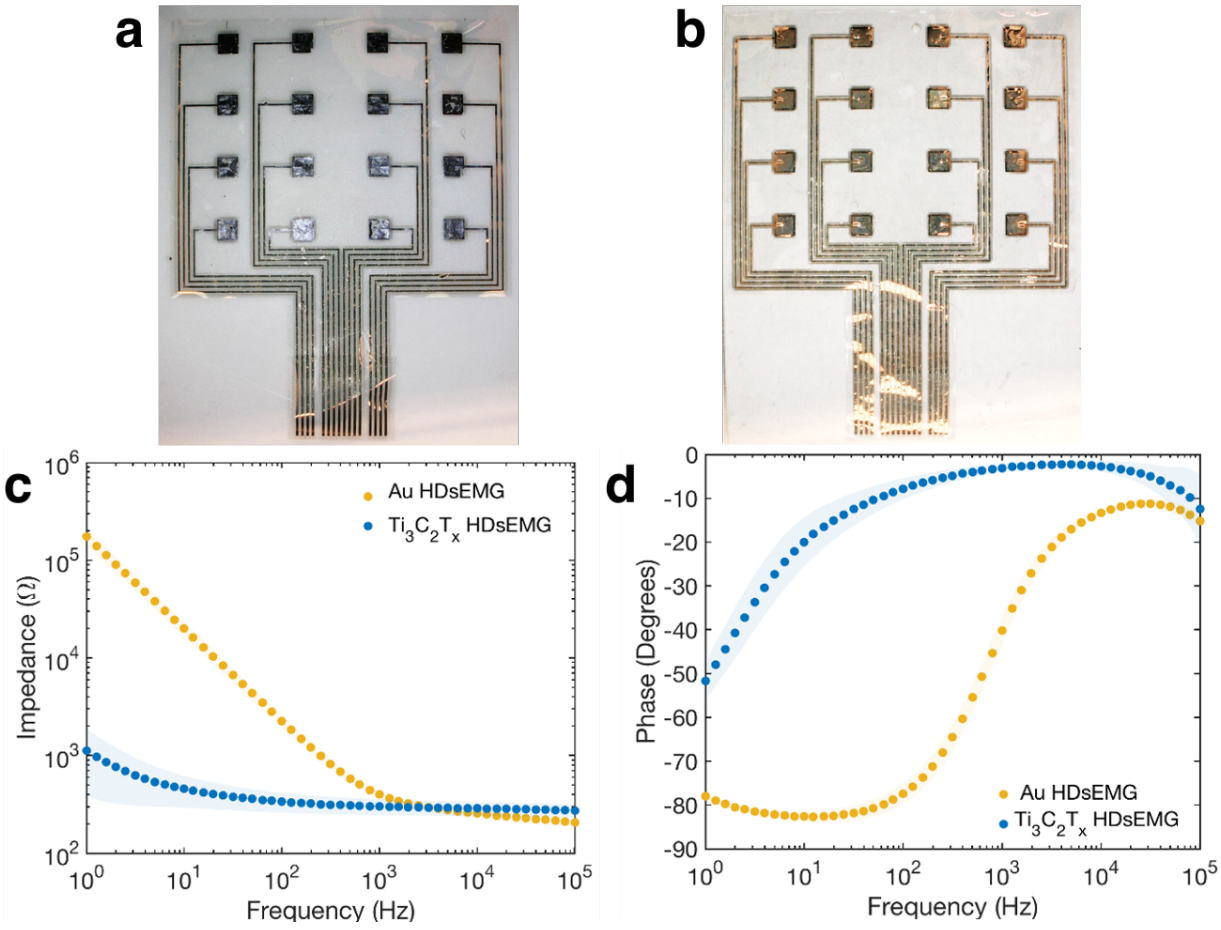

Figure S1 Imaging and EIS Characterization of $Ti_3C_2T_x$ HDsEMG arrays in 10 mM PBS (pH 7.4). **a, b)** Light microscopy images of a) $Ti_3C_2T_x$ and b) Au 16-channel HDsEMG arrays. **c, d)** Bode plot of c) impedance modulus and d) phase of the $Ti_3C_2T_x$ and Au HDsEMG arrays in PBS. Points represent means, shaded areas show the standard deviations. $n_{Ti3C2Tx} = n_{Au} = 16$ channels.

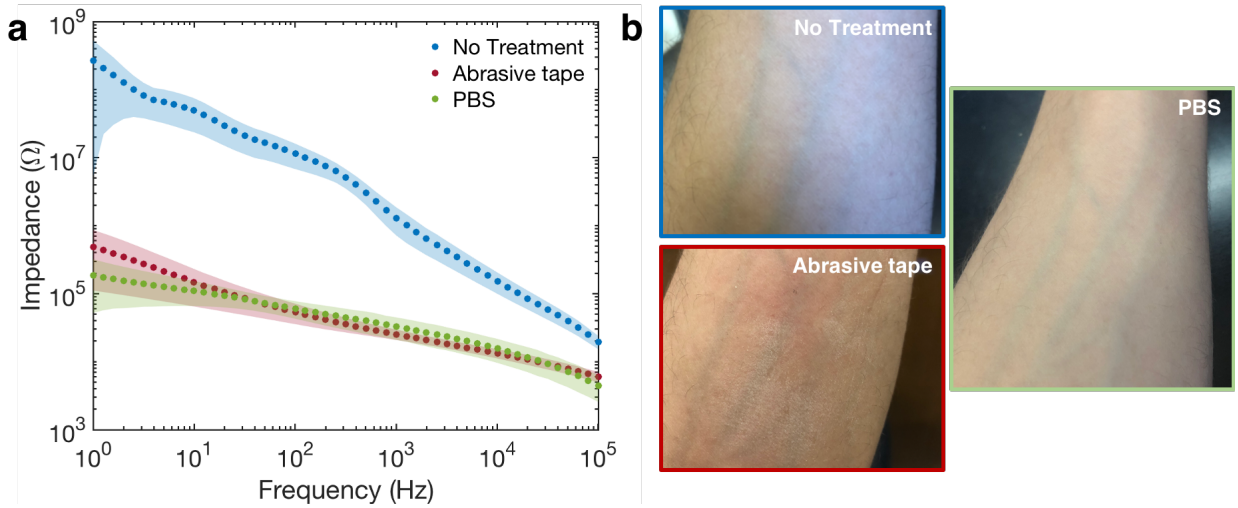

Figure S2 Effect of the skin treatment on the impedance of the $Ti_3C_2T_x$ arrays. **a)** Bode plot of the impedance modulus under the different treatments tested. 'No treatment': skin was only cleaned with an alcohol prep pad. 'Abrasive tape': skin was cleaned and abraded with 3M Trace Prep abrasive tape. 'PBS': skin was cleaned, then a few drops of PBS were applied to the skin surface and the $Ti_3C_2T_x$ array was immediately placed. Points represent means, shaded areas are standard deviations. n = 8 channels for each treatment. **b)** Images of the skin directly under the array for each treatment after EIS recordings. Images are bordered with colors corresponding to the specific skin treatment.

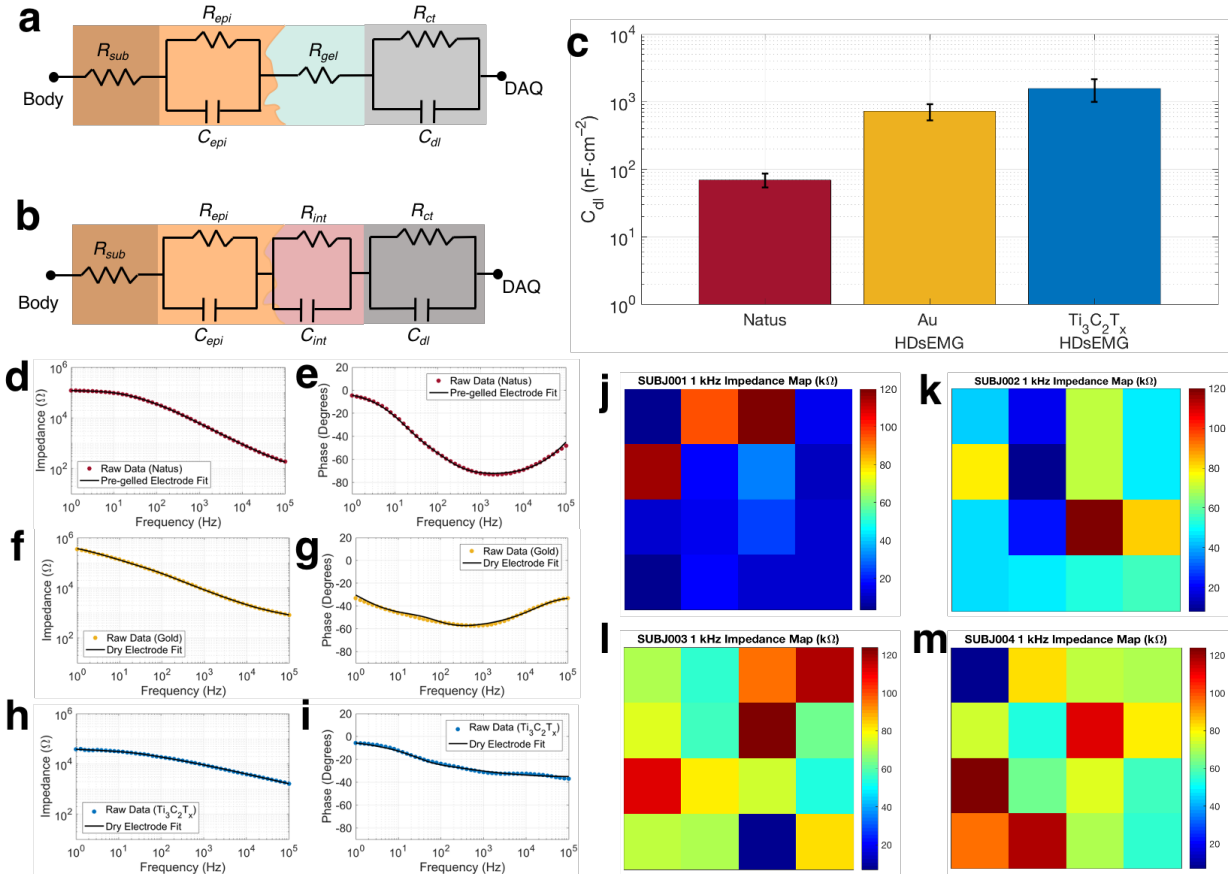

Figure S3 Characterization of the skin-electrode interface. **a, b)** Equivalent circuit models[69,70] for a) the Natus pre-gelled Ag/AgCl electrodes and b) the Au and $Ti_3C_2T_x$ dry HDsEMG arrays. R_{sub} is the subcutaneous resistance; R_{epi} and C_{epi} are the epidermal resistance and epidermal capacitance, respectively; R_{gel} is the resistance of the Natus electrolytic gel; R_{int} and C_{int} are the interfacial resistance and interfacial capacitance, respectively; R_{ct} is the charge-transfer resistance, and C_{dl} is the double-layer capacitance. **c)** Double-layer capacitance as determined by fitting the impedance spectra of Natus, Au HDsEMG, and $Ti_3C_2T_x$ HDsEMG contacts (n = 4 separate contacts for each type of electrode measured on 3 different subjects). Note the logarithmic scale. See Table S1 for values of the other fitting parameters. **d–i)** Bode plots of the impedance modulus and phase for a representative d, e) Natus contact, f, g) channel of the Au HDsEMG array, and h, i) channel of the $Ti_3C_2T_x$ HDsEMG array. The solid black lines in each plot represent fitted impedance. **j–m)** Distribution of the impedance magnitude at 1 kHz on the $Ti_3C_2T_x$ HDsEMG arrays, for each of the subjects, at the start of the recording session over their *thenar eminence*.

Table S1 Values of the fitted parameters in the skin-electrode impedance model. The Natus electrode impedance was fitted using the pre-gelled skin electrode equivalent circuit model (Figure S3a), while the impedance of the Au and $Ti_3C_2T_x$ HDsEMG contacts were fitted using the dry skin electrode equivalent circuit (Figure S3b). The equivalent circuit models were built, and all subsequent fitting was completed, using Gamry's *EChem Analyst* software package. For all fits, R_{sub} was limited in the 10–100 Ω cm^2 interval, and the values of R_{epi} and C_{epi} were limited within 10 kΩ cm^2 – 1 MΩ cm^2, and 10–90 nF cm^{-2}, respectively.[70] The values of R_{gel} and R_{int} were given an upper bound of 10 kΩ cm^2, and C_{int} was given an upper bound of 90 nF cm^{-2}. R_{ct} and C_{dl} were only given a lower bound (0 Ω cm^2 and 0 nF cm^{-2}, respectively). These bounds were determined from literature, and according to the high- and low-frequency behavior of the total equivalent impedance for each of the equivalent circuit models explored. Values in Table are mean ± S.D.

Electrode	**GSA [cm^2]**	R_{sub} **[kΩ cm^2]**	R_{epi} **[kΩ cm^2]**	C_{epi} **[nF cm^{-2}]**	R_{gel} **[kΩ cm^2]**
Pre-gelled Ag/AgCl (Natus)	0.8	0.047 ± 0.013	48.34 ± 8.06	50.42 ± 20.45	0.08 ± 0.01
Au HDsEMG	0.0256	0.026 ± 0.008	21.89 ± 7.19	34.03 ± 6.39	—
$Ti_3C_2T_X$ HDsEMG		0.026 ± 0.005	29.78 ± 8.18	23.68 ± 12.22	

Electrode	**GSA [cm^2]**	R_{int} **[kΩ cm^2]**	C_{int} **[nF cm^{-2}]**	R_{ct} **[kΩ cm^2]**	C_{dl} **[nF cm^{-2}]**	χ^2 **[×10^3]**
Pre-gelled Ag/AgCl (Natus)	0.8	—		51.55 ± 22.61	69.52 ± 16.18	8.03 ± 1.15
Au HDsEMG	0.0256	1.09 ± 0.29	16.69 ± 7.72	1.07 ± 0.81	724.32 ± 192.40	23.44 ± 4.04
$Ti_3C_2T_X$ HDsEMG		0.48 ± 0.28	16.98 ± 5.52	0.51 ± 0.29	1,568.65 ± 579.52	6.24 ± 1.39

Table S2 Signal-to-noise ratios (SNRs) for each type of electrode, for sEMG recordings over the *flexor digitorum superficialis*. n_{tasks} is the number of completed contraction tasks for each subject. The SNRs given for the $Ti_3C_2T_x$ and Au arrays are the averages of the epochal SNRs across all 16 channels in the HDsEMG arrays for all of the n_{tasks} following Equation 1 in the main text. The SNRs given for the Natus contacts are the averages of the epochal SNRs calculated for a single electrode, over all of the completed n_{tasks}.

		SNR [dB]		
SUBJ###	n_{tasks}	**$Ti_3C_2T_x$ HDsEMG**	**Au HDsEMG**	**Natus**
001	10	39.23 ± 16.25	12.54 ± 7.35	8.72 ± 4.69
002	12	24.41 ± 1.67	19.13 ± 2.74	10.99 ± 3.63
003	5	19.33 ± 4.23	16.57 ± 1.99	Not recorded

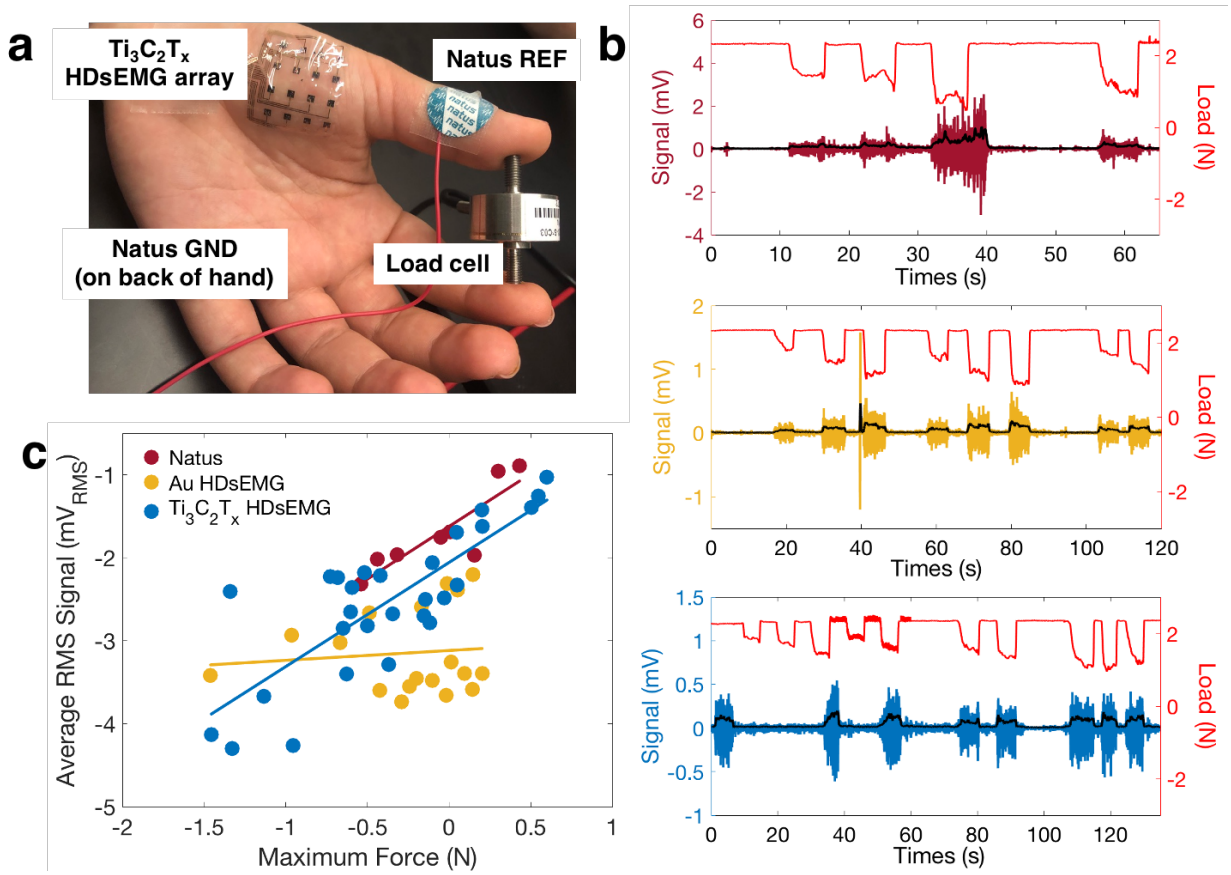

Figure S4 Correlation of sEMG signals and loading force for all subjects. **a)** Experimental setup, showing the working electrode placed over the *thenar eminence*, as well as the load cell being pinched between the thumb and forefinger. **b)** Representative plots of the exerted force (top trace in each plot, in red) and the recorded sEMG (bottom traces in each plot) over time for (from top to bottom): a single Natus contact, a single channel of the Au HDsEMG, and a single channel of the $Ti_3C_2T_x$ HDsEMG. The RMS envelope of the sEMG signals is overlaid on the raw data in black. **c)** Scatter plot of the average RMS signal from the sEMG recordings versus the maximum exerted force in that epoch. Points represent individual pinches from all subjects. Lines were fitted to the data on a log-log scale, for each of the electrode types, to characterize the sensitivity of the electrode material at resolving changing levels of force exertion (Table S3), following from Equation 3 in the main text.

Table S3 Correlation of the RMS envelope from sEMG recordings to force levels of exertion across different materials and electrode designs. n_{Events} is the number of pinching events considered in this analysis across all four of the recruited subjects. Sensitivity was determined from fitting a line to the log-log plot of the average RMS signal versus the maximum force (Figure S4c). The GSA-normalized sensitivity was determined by dividing the sensitivity of each electrode by its geometric surface area.

Electrode	**GSA [cm^2]**	n_{Events}	**Sensitivity [$mV_{RMS}\ N^{-1}$] (from linear fit)**	R^2	**GSA-Normalized Sensitivity [$mV_{RMS}\ N^{-1}\ cm^{-2}$]**
Pre-gelled Ag/AgCl (Natus)	0.8	8	1.27	0.9184	1.59
Au HDsEMG	0.0256	18	0.12	0.8557	4.69
$Ti_3C_2T_X$ HDsEMG		28	1.25	0.9097	49.61